Study on vacuum consolidation combined with embankment loading through centrifuge model tests and its a 3D FEM analysis

Shinichirou Shiraga[1], G. Hasegawa[2], Y. Sawamura[2], and M. Kimura[2]

[1] Kinjo Rubber Corporation Limited, Yao-shi, Osaka, 581-0068, Japan.
[2] Department of Civil and Earth Resource Engineering, Kyoto University, Nishikyo-ku, Kyoto, 615-8540, Japan.

ABSTRACT

Vacuum consolidation is a method of consolidating soft clays by applying vacuum pressure through installed drains. This method stabilizes soft clays without shear deformation, so a combination of vacuum consolidation and embankment loading is widely used. However, there are some unclear points regarding the pore water pressure behavior during vacuum consolidation. In this study, centrifuge model tests and a numerical analysis were conducted focusing on the mechanical behavior around a drain. The centrifuge model tests revealed that there was a greater increase in negative pressure in areas closer to the drain, and that the increase in water pressure during embankment loading was suppressed in those areas. Furthermore, the numerical analysis indicated that the stability effect of the ground by embankment loading prior to vacuum consolidation was not effective when the improvement area was too broad for the drain.

Keywords: vacuum consolidation; embankment loading; centrifuge modeling; numerical simulation

1 INTRODUCTION

Figure 1 shows an outline of the vacuum consolidation method. On a ground to which vacuum consolidation is applied, negative pressure rapidly propagates through the drainage material, and it is possible for the ground to consolidate without causing shear deformation. Much research has been conducted with two-dimensional FEM analyses under plane strain conditions to verify the behavior of the ground, such as settlement, pore water pressure and lateral displacement, using vacuum consolidation in combination with embankment loading (e.g., Nguyen et al., 2015). However, some unclear points remain with the pore water pressure and the lateral displacement in the ground during vacuum consolidation combined with embankment loading. Thus, centrifugal model tests, focusing on the stress condition around an installed drain, and a 3D FEM analysis were carried out in this study to clarify the stabilizing effect during embankment loading by vacuum consolidation.

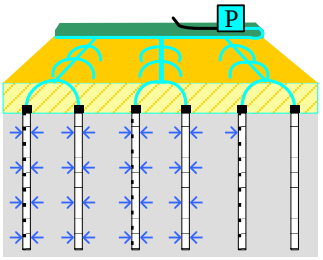

Fig. 1. Outline of vacuum consolidation method.

2 CENTRIFUGE MODEL TESTS

2.1 Test cases of centrifuge modeling

Centrifuge model tests (Shiraga et al., 2018) were conducted for three cases at an acceleration of 50 g. Case-1 is embankment loading only, Case-2 is vacuum consolidation combined with embankment loading with prior vacuum consolidation and Case-3 is vacuum consolidation combined with embankment loading without prior vacuum consolidation. The distribution of water pressure around the drain is evaluated for each case.

2.2 Overview of tests

Figure 2 shows the schematics of Case-2 and Case-3. All of the conditions for Cases-1, -2 and -3 were completely the same, except for the drain. In this experiment, Fujinomori clay was used for the clay ground, and the clay slurry was adjusted to be 1.5 times greater than the liquid limit. Embankment loading was simulated by an air cylinder and a loading plate. The load and the loading speed were the same in all cases, and an equally distributed load of 54 kPa, in terms of the prototype, was loaded one-dimensionally at a loading speed of 0.9 kPa/day. As shown in Figure 3, vacuum consolidation was simulated by applying negative pressure to the inside of a model drain installed in the center of the ground with a vacuum pump.

3 SOIL/WATER COUPLED FEM ANALYSIS

3.1 Overview of analysis

In the reproduction analysis of the centrifugal model tests, a three-dimensional soil/water coupled analysis was performed using the elasto-plastic finite element analysis code DBLEAVES (Ye et al., 2007). Figure 4 shows the analytical mesh. The x-y cross section of the clay ground was modeled with a size of 1/4. The initial stress of each element was taken as the load by the loading plate as the vertical stress, and the horizontal stress was obtained from the coefficient of earth pressure at rest. The embankment load was simulated by giving a predetermined nodal load to the node at the top of the mesh. Vacuum consolidation was reproduced by the acting negative pressure, whose value was the mean value of the test at the element boundary corresponding to the circumferential surface of the drain.

3.2 Analysis model

In this analysis, the subloading t_{ij} model (Nakai and Hinokio, 2004), one kind of elastic plasticity model, was applied. In this model, it is possible to consider the influence of the intermediate main stress and the depend ency of the shear rigidity on the restraint pressure. Moreover, this model can be applied to both the normal consolidation state and the over consolidation state without making a distinction between sand and clay. Table 1 shows the parameters of the Fujinomori clay used here. The principal stress ratio at critical state R_{cs}, density coefficient a and dilatancy coefficient β were determined based on past research, and the other parameters were obtained from the results of standard consolidation tests.

4 RESULTS OF EXPERIMENT AND ANALYSIS

The following results are written in prototype scale. The vertical pressure and excess pore water pressure are corrected based on the changes in the water level in the box.

4.1 Water level and negative pressure

Figure 5 shows the changes in water pressure in the water layer and the drain in Case-2 and Case-3. The water level started decreasing from the start of vacuum application and kept decreasing until the end of the test. It is thought that negative pressure propagated to the ground surface by vacuum consolidation and that the water in the water layer flowed into the drain. From this fact, it is considered that the seepage flow occurred from the ground surface toward the drain in this experiment. When vacuum consolidation was started, the negative pressure acting on the drain rapidly increased, but it decreased as time passed. It is suggested that the head loss occurred due to the difference in elevation between the drainage hose and the water surface caused by the lowering of the water level.

4.2 Embankment load and vertical pressure

Figure 6 shows the changes in the embankment load and the vertical earth pressure at the bottom of the clay layer in Case-1. The pressure is calculated by dividing

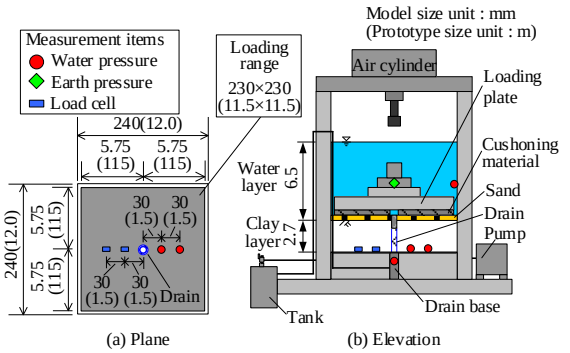

Fig. 2. Schematic of centrifuge model tests (Case-2 and Case-3).

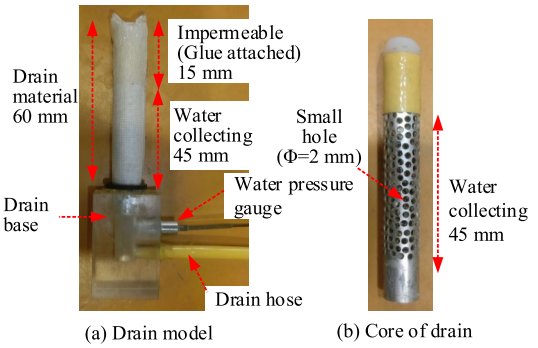

Fig. 3. Drain model.

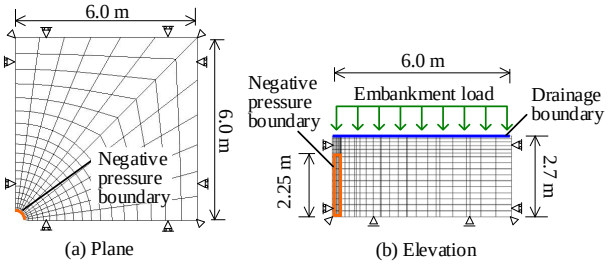

Fig. 4. Analytical mesh and boundary conditions.

Table 1. Parameters of Fujinomori clay.

Property	Value
Unit volume weight γ_t [kN/m^3]	15.7
Principal stress ratio at critical state $Rcs = (\sigma_1/\sigma_3)_{cs(comp.)}$	3.5
Compression index λ	0.113
Swelling index κ	0.01
Poisson's ratio ν	0.333
Coefficient of earth pressure at rest K_0	0.5
$N = e_{NC}$ at p = 98 kPa & q = 0 kPa	0.847
Density coefficient a	500
Dilatancy coefficient β	1.5
Hydraulic conductivity k [m/s]	4.2×10^{-9}
Slope of e-ln k λ_k	0.26

the load measured in the load cell by the area of the loading plate (11.5 m × 11.5 m). Embankment loading was completed in about 55 days and a load of about 55 kPa was loaded on the ground surface. After the end of

loading, a pressure of 54~55 kPa was maintained during consolidation. In addition, the vertical pressure at the bottom of the ground increased by about 60 kPa at both measuring points. The increments in the embankment load and the vertical pressure were almost the same; it is seen that an even load was simulated in this model. The same results were obtained for Case-2 and Case-3.

4.3 Pore-water pressure

Figure 7 shows the change in excess pore water pressure at the bottom of clay layer for each case. The experimental values are indicated by solid lines and the numerical analysis values are indicated by broken lines.

Regarding the test values, Figure 8(a) shows that the water pressure in Case-1 tended to increase more in areas closer to the center of the ground. This is because friction occurred between the side wall of the box and the ground, and the influence of friction became smaller in areas closer to the center of the ground. Figure 8(b) shows that the water pressure in Case-2 decreased when vacuum consolidation was started and the propagation amount of negative pressure became larger closer to the drain. After that, when embankment loading had started, the water pressure increased. The results of Case-1 show that the increase in pore water pressure during embankment loading was greater in regions closer to the center of the ground due to friction between the side wall and the soil. In Case-2, however, the increase in water pressure during embankment loading was smaller in regions closer to the drain installed at the center of the ground. These results indicate that the suppression of the increase in pore water pressure was greater in regions closer to the drain material during vacuum consolidation combined with embankment loading. As shown in Figure 8(c), it was confirmed that the increase in water pressure due to the embankment loading was suppressed in Case-3, as it was in Case-2, because it was closer to the drain.

Regarding the numerical analysis, Figure 7(a) shows that the increment in water pressure by embankment loading exceeded the experimental value in Case-1, but that the water pressure in the experiment was almost reproduced. Figure 7(b) shows that the propagation process of negative pressure was reproduced well in the prior vacuuming period in Case-2. As shown in Figures 8(b) and (c), it was possible to reproduce the water pressure of the experiment during embankment loading well in the element 3.0 m from the center of the drain, but the results for the element 1.5 m from the center of the drain were lower than the experimental values. Furthermore, after the completion of embankment loading, the dissipation of excess pore water pressure in the analysis was much faster than that in the experiment. In the experiment, it is thought that the seepage flow occurred from the ground surface toward the drain; therefore, water was less likely to flow from the ground surface during embankment loading. Although the influence of the seepage flow was not considered in the analysis, we concluded from these results that the propagation process of the negative pressure in the ground combined with the vacuum consolidation and the embankment loading and the water pressure behavior during the embankment loading can be reproduced.

Fig. 5. Water pressure in the water layer and the drain.

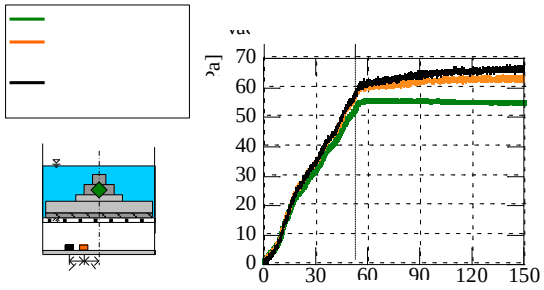

Fig. 6. Embankment load and earth pressure (Case-1).

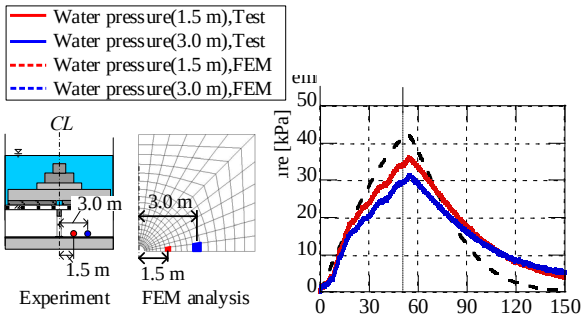

(a) Case-1

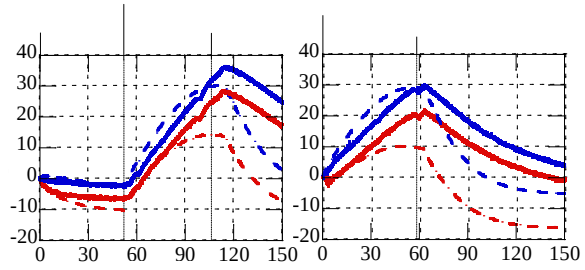

(b) Case-2 (c) Case-3

Fig. 7. Excess pore water pressure at the bottom of clay layer (Case -1, Case-2 and Case-3).

5 ANALYSIS WITH THE SAME ACTING NEGATIVE PRESSURE

In the experiment, the negative pressure acting on the drain was different between Case-2 and Case-3. Therefore, an analysis follows in which the acting negative pressure of Case-2 is set to be the same as that of Case-3 (average value of -53.0 kPa). Case-2, in which the negative pressure has been changed, is denoted as Case-2'. Figure 8 shows the distribution of excess pore water pressure in each case. The water pressure distribution on the 10th day after the start of embankment loading was larger for Case-3 than for

Case-2', but the distribution at the completion of embankment loading was almost the same for Case-2' and Case-3. Figure 9 shows the distribution of effective stress in each case. From the distribution at the completion of embankment loading, it is found that the effective stress increased more than the embankment load (55 kPa) and the acting negative pressure (-53.0 kPa) in the vicinity of the drain, and that stress concentration occurred. In addition, similar to the water pressure distribution, the effective stress distributions of Case-2' and Case-3 were almost the same at the completion of embankment loading. These results show that when the improvement area was too large for the drain, the differences in the distributions of water pressure and effective stress in the case of the combined use, with and without prior vacuuming, became smaller as the embankment load increased. The following two scenarios are conceivable, but further study will be necessary in the future.

1. Before embankment loading, the water pressure decreased as it approached the drain in Case-2', so the hydrodynamic gradient between the drain and the clay on embankment loading was larger in Case-3 than in Case-2'. Therefore, the pore water pressure tended to increase more in Case-2' than in Case-3.
2. In Case-2', there was a range that had not propagated before embankment loading. Since the range where the rigidity was increased by the negative pressure was sandwiched between the drain and the rigidity in the initial state, water flowed in from the initial stiffness range, and water pressure was likely to have increased in the range where the negative pressure propagated at the embankment load.

6 SUMMARY

In this study, centrifugal model tests, focusing on the stress state around installed a drain, and a 3D analysis of the tests were conducted. The obtained findings are given below.

1. In the centrifugal tests, it was confirmed that when the vacuum consolidation method was combined with embankment loading, the propagation amount of the negative pressure became larger closer to the drain, and the increase in water pressure decreased during embankment loading.
2. In the numerical analysis of the tests, it was possible to roughly reproduce the hydraulic behavior of the negative pressure propagation process and the embankment load. The validity of the analysis in this study was confirmed.
3. Comparing the analysis of Case-2' and Case-3, when the improvement area was too large for the drain, the differences in the distributions of water pressure and effective stress became smaller as the completion of embankment loading approached.

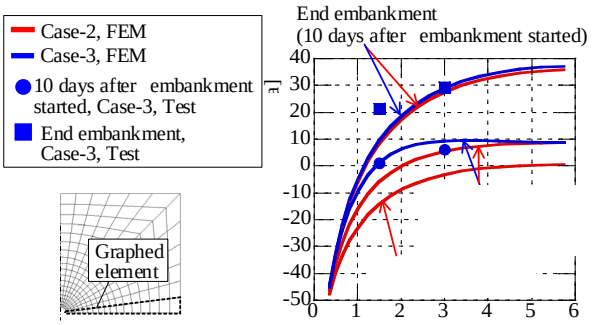

Fig. 8. Distribution of excess pore water pressure.

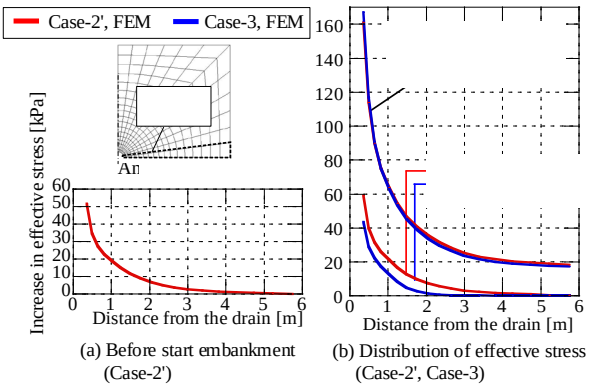

Fig. 9. Distribution of effective stress.

REFERENCES

Nakai, T. and Hinokio, M. (2004). A simple elastoplastic model for normally and over consolidated soils with unified material parameters. Soils and Foundations, 44(2), 53-70.

Nguyen, HS., Tashiro, M., Inagaki, M. and Noda, T. (2015). Simulation and evaluation of improvement effects by vertical drains/vacuum consolidation on peat ground under embankment loading based on a macro-element method with water absorption and discharge functions. Soils and Foundations, 55(5), 1044–1057.

Shiraga, S., Hasegawa, G., Sawamura, Y. and Kimura, M. (2018). Centrifuge model test of vacuum consolidation on soft clay combined with embankment loading. 9th International Conference on Physical Modelling in Geotechnics, 1067-1072.

Ye, B., Ye, G. L., Zhang, F. and Yashima, A. (2007). Experiment and numerical simulation of repeated liquefaction-consolidation of sand. Soils and Foundations, 47(3), 547-558.